Published in final edited form as:
Synapse. 2009 September ; 63(9): 717–728. doi:10.1002/syn.20652.

[^{3}H]4-(Dimethylamino)-N-[4-(4-(2-methoxyphenyl)piperazin-1-yl)butyl]benzamide, a Selective Radioligand for Dopamine D_3 receptors. II. Quantitative Analysis of Dopamine D_3 and D_2 Receptor Density Ratio in the Caudate-putamen

Jinbin Xu[1], **Babak Hassanzadeh**[1], **Wenhua Chu**[1], **Zhude Tu**[1], **Lynne A. Jones**[1], **Robert R. Luedtke**[6], **Joel S. Perlmutter**[1,4], **Mark A. Mintun**[1,5], and **Robert H. Mach**[1,2,3,*]

[1] Department of Radiology, Washington University School of Medicine, 510 S. Kingshighway Blvd., Saint Louis, MO 63110, USA

[2] Department of Cell Biology and Physiology, Washington University School of Medicine, 510 S. Kingshighway Blvd., Saint Louis, MO 63110, USA

[3] Department of Biochemistry and Molecular Biophysics, Washington University School of Medicine, 510 S. Kingshighway Blvd., Saint Louis, MO 63110, USA

[4] Department of Neurology, Washington University School of Medicine, 510 S. Kingshighway Blvd., Saint Louis, MO 63110, USA

[5] Department of Psychiatry, Washington University School of Medicine, 510 S. Kingshighway Blvd., Saint Louis, MO 63110, USA

[6] Department of Pharmacology and Neuroscience, University of North Texas Health Science Center, Fort Worth, TX 76107, USA

Abstract

4-(Dimethylamino)-*N*-(4-(4-(2-methoxyphenyl)piperazin-1-yl)butyl)benzamide (**WC-10**), a *N*-phenyl piperazine analog, displays high affinity and moderate selectivity for dopamine D_3 receptors versus dopamine D_2 receptors (Chu et al. [2005] Bioorg. Med. Chem. 13; 77–87). In this study, **WC-10** was radiolabeled with tritium (specific activity = 80 Ci/mmol) and quantitative autoradiography studies were conducted using rhesus monkey and Sprague-Dawley rat brain sections. K_d values for the binding of [^{3}H]**WC-10** to D_3 receptors obtained from quantitative autoradiography with rhesus monkey and rat brain sections are in agreement with K_d values obtained from cloned human and rat receptors (Xu et al., 2009). The D_2 selective antagonist [^{3}H]raclopride binds with 11-fold higher affinity to human HEK D_{2L} (K_d = 1.6 nM) than HEK D_3 (K_d = 18 nM) receptors; and [^{3}H]raclopride binds to rat Sf9 rD_{2L} receptors with a K_d of 6.79 nM, a value that is 4-fold lower than binding to human HEK D_{2L} receptors and 2.5-fold higher than binding to rat Sf9 rD_3 receptors. *In vitro* quantitative autoradiography studies with [^{3}H]**WC-10** and [^{3}H]raclopride were conducted on adult rat and rhesus monkey brain sections. A mathematical model for calculating the absolute densities of dopamine D_2 and D_3 receptors based on the *in vitro* receptor binding data of [^{3}H]**WC-10** and [^{3}H]raclopride was developed.

*Address correspondence to: Robert H. Mach, Ph.D., Division of Radiological Sciences, Mail Box 8225, Washington University School of Medicine, 510 S. Kingshighway Blvd., Saint Louis, MO 63110, rhmach@mir.wustl.edu, Phone: (314) 362-8538, Fax: (314) 362-0039.

Keywords

dopamine D_3/D_2 receptors; quantitative autoradiography

INTRODUCTION

$D_{1\text{-like}}$ and $D_{2\text{-like}}$ receptor subtypes are the two major classes of dopamine receptors. The $D_{1\text{-like}}$ receptor subtypes include the D_1 (D_{1a}) and D_5 (D_{1b}) receptors and stimulation of $D_{1\text{-like}}$ receptors activates adenylate cyclase. The $D_{2\text{-like}}$ receptor subtypes consist of the D_2 (both long and short isoforms), D_3, and D_4 receptors. Agonist stimulation of $D_{2\text{-like}}$ receptors a) inhibits adenylate cyclase activity and b) increases the release of arachadonic acid and phosphatidylinositol hydrolysis (Luedtke and Mach, 2003; Neve et al., 2004).

$D_{2\text{-like}}$ receptors exist in two interconvertible affinity states for their natural agonist dopamine: a high-affinity state and a low-affinity state (Sibley et al., 1982). Under physiological conditions, dopamine binds predominantly to the high affinity state and mediates the activation of the second-messenger cascade. Although autoradiography studies using the D_2/D_3 agonists, [^{3}H]7-OH-DPAT and [^{3}H]quinpirole, under conditions minimizing binding to the D_2 receptor, suggest that dopamine D_3 receptors are localized in the ventral striatum and the Islands of Calleja (Gehlert et al., 1992; Kaichi et al., 2000; Levesque et al., 1992), there are data indicating that the density of dopamine D_3 receptors measured with agonists [^{3}H]7-OH-DPAT and [^{3}H]PD128907 is higher in the adult rat caudate–putamen than in the islands of Calleja (Hillefors and von Euler, 2001; Hillefors et al., 1999). The high affinity state is believed to be the functionally important state (George et al., 1985; Leff, 1995). Nevertheless, the low affinity state of $D_{2\text{-like}}$ receptors, and its conversion to a high affinity state, needs to be further investigated in evaluating their regulatory functions in both diseased and healthy individuals (Briand et al., 2008; Graff-Guerrero et al., 2009; King et al., 2009; Skinbjerg et al., 2009).

It has been difficult to obtain ligands specifically selective for D_2 or D_3 receptors due to the high degree of amino acid homology in the helical transmembrane spanning regions of those receptors. Some selective dopamine D_3 agonists (7-OH-DPAT and PD128947) and dopamine D_2 agonists (PHNO) are available, but selective D_2 or D_3 receptor antagonists are not well documented (Ginovart et al., 2006; Luedtke and Mach, 2003; Vasdev et al., 2007). The development of high affinity D_3 and D_2 receptor antagonists would be valuable for studying the regulating mechanism of these receptors in neurological disorders.

A *N*-phenyl piperazine analog, 4-(dimethylamino)-*N*-(4-(4-(2-methoxyphenyl)piperazin-1-yl)butyl)benzamide (**WC-10**), displays higher affinity and binding selectivity for dopamine D_3 receptors versus dopamine D_2 receptors (Chu et al., 2005). In a previous publication, **WC-10** was radiolabeled with tritium (specific activity = 80 Ci/mmol) and the binding of [^{3}H]**WC-10** to genetically cloned human and rat dopamine D_{2L} and D_3 receptors was evaluated *in vitro* (Xu et al., 2009). *In vitro* autoradiography studies showed that [^{3}H]**WC-10** specifically labeled the D_3 sites of striatum in adult Sprague-Dawley rat and rhesus monkey brains. In this paper, saturation binding with [^{3}H]**WC-10** was carried out to evaluate the binding affinity (K_d) with quantitative autoradiography. Comparatively, we characterized D_2 selective antagonist [^{3}H]raclopride binding properties at D_2 or D_3 receptors. *In vitro* quantitative autoradiography studies combining the D_3/D_2 ligand, [^{3}H]**WC-10** and the D_2/D_3 ligand, [^{3}H]raclopride, were also conducted on adult rat and rhesus monkey brain sections. A mathematical model for calculating the absolute densities of dopamine D_2 and D_3 receptors based on the *in vitro* binding data obtained from

[^{3}H]**WC-10** and [^{3}H]raclopride was also developed and used to determine the density of D_2 and D_3 dopamine receptors.

MATERIALS AND METHODS

Precursor synthesis and radiolabeling

[^{3}H]**WC-10** (Fig. 1) was synthesized by American Radiolabeled Chemicals, Inc. (St. Louis, MO, U.S.A.) by alkylation of the des-methyl precursor with [^{3}H]methyl iodide. The specific activity of the radioligand was 80 Ci/mmol. The detailed synthesis scheme for [^{3}H]**WC-10** was reported (Xu et al., 2009).

Drugs and preparation

Chemical reagents and the standard compounds were purchased from Sigma (St. Louis, MO) and Tocris (Ellisville, MO). Novel compounds used in this study were synthesized by our group. *N*,*N*-Dimethylformamide (DMF), dimethyl sulfoxide (DMSO) or ethanol were used to dissolve the various compounds to 3 mM as stock solutions. Different concentrations were then achieved by diluting stock solutions with a solution containing 50 mM Tris-HCl, 150 mM NaCl and 100 mM EDTA at pH 7.4. The final solvent volume in the dilutions was less than 0.1% of the total volume. [^{3}H]raclopride (60.1 Ci/mmol) was purchased from Pekin Elmer Life Sciences (Boston, MA).

Membrane homogenate preparation

HEK or Sf9 cells expressing human or rat D_2 and D_3 receptors were harvested by centrifugation at 6,000*g* for 10 min (Luedtke et al., 2000). The cell pellet was resuspended in cold (4°C) homogenization buffer (50 mM Hepes, pH 7.4, 0.1 mM EDTA, 1 mM DTT) by vigorous vortexing and then homogenized using an Ultra-Turrax T8 polython homogenizer (IKA Works, Inc, Wilmington, NC). The homogenate was centrifuged at 40,000*g* for 10 min at 4°C and the resulting crude membrane pellet was resuspended in homogenization buffer. Aliquots were stored at −80°C until used. The protein concentration of the suspension was determined using the DC protein assay (Bio-Rad, Hercules, CA) and averaged 1~2 mg of protein/ml of stock solution.

Radioligand binding assay

Scatchard analysis of [^{3}H]raclopride binding to receptor membrane homogenates—Membrane homogenates were diluted and incubated for 60 min with the radioligand [^{3}H]raclopride in a total volume of 150 μl at 25°C in 96-well polypropylene plates (Fisher Scientific, Pittsburgh, PA). The amount of protein added to each well was 10~20 μg for genetically cloned D_{2L} and D_3 receptors. The concentrations of the radioligand ranged from 0.1 to 30.0 nM, reactions were terminated by the addition of 150 μl of cold wash buffer (10 mM Tris-HCl, 150 mM NaCl, pH 7.4, at 4°C) using a 96-channel transfer pipette (Fisher Scientific, Pittsburgh, PA), and the samples were harvested and filtered rapidly to 96-well fiberglass filter plate (Millipore, Billerica, MA) that had been presoaked with 100 μl of 50 mM Tris-HCl buffer, pH 8.0 for 1 hour. Each filter was washed with 200 μl of ice-cold wash buffer for a total of three washes and 150 μl of scintillation fluid was added in each well. A Wallac 1450 MicroBeta liquid scintillation counter (Perkin Elmer, Boston, MA) was used to quantitate the bound radioactivity. Nonspecific binding was determined from samples which contained 10 μM haloperidol.

The equilibrium dissociation constant (K_d) and maximum number of binding sites (B_{max}) were determined by a linear regression analysis of the transformed data using the method of Scatchard (Scatchard, 1949).

Data from saturation radioligand binding studies were transformed to determine the Hill coefficient, n_H, defined as:

$$\log\frac{B_s}{B_{\max}-B_s} = -\log K_d + n_H \log L \quad (1)$$

(Hill 1910; McGonigle and Molinoff, 1989). L is the concentration of radioligand. n_H, Hill slope, was determined from a Hill plot of $\log\frac{B_s}{B_{\max}-B_s}$ versus log L.

Scatchard analysis of autoradiography binding assay with [^{3}H]WC-10 to rhesus monkey and rat brain sections—Rhesus monkey and rat brain adjacent sections were incubated with [^{3}H]**WC-10,** with concentration ranging from 0.5 to 16.0 nM. Quantitative imaging analysis for the anatomical regions of interest (ROI), caudate and putamen, was performed using a Beta Imager 2000Z Digital Beta Imaging System. Scatchard binding analysis were carried out as described in the previous section. Nonspecific bond activity at each concentration was defined from slides using 1 uM S(−)-Eticlopride.

Quantitative autoradiography

Intact brains from ~500 g male Sprague-Dawley rats at age of 5 months and a 5 kg male rhesus monkey at age of 6 years (euthanized due to a pancreatic tumor) were flash frozen in dry ice, pre-cooled in isopentane and stored at −80°C until used. Coronal sections (20 μm) were cut with a Microm cryotome and mounted on superfrost plus glass slides (Fisher Scientific, Pittsburgh, PA). Sections were incubated with 4 nM of [^{3}H]**WC-10** or 10 nM of [^{3}H]raclopride in the same buffer used for binding assays, in the presence or absence of 1 μM cold S(−)-Eticlopride (to define nonspecific binding) for 30 minutes, and then rinsed 5 times at one minute intervals each time with ice-cold buffer. Slides were incubated in the wide open staining jar, and the free radioligand concentration loss was less than 5% after ligands bound to brain sections. Slides were dried and made conductive by coating the free side with a copper foil tape. Slides were then placed in the gas chamber [mixture of argon and triethylamine (Sigma–Aldrich, USA)] of a gaseous detector system, the Beta Imager 2000Z Digital Beta Imaging System (Biospace, France). After the gas was well mixed and a homogenous state was reached, further exposure for 24 hours yielded high quality images. [^{3}H]Microscale (American Radiolabeled Chemicals, Inc., St. Louis, MO) was counted at the same time as a reference for total radioactivity quantitative analysis. Quantitative analysis was performed with the program Beta-Vision Plus (BioSpace, France) for the anatomical regions of interest (ROI).

In comparison with digital Beta Imager, the dried slides with brains sections were also exposed to a ^{3}H-sensitive film (^{3}H-Hyperfilm, Amersham, Buckinghamshire, UK) for 1 or 3 months, and the film was developed with a Kodak X-OMAT 2000A processor.

Determination of absolute densities ratio of D_2 and D_3 receptors from autoradiography studies

[^{3}H]**WC-10** and [^{3}H]raclopride bind to dopamine D_2 and D_3 receptors with different labeling proportions. Based upon receptor homogenates binding studies, 4 nM [^{3}H]**WC-10** will label 2% of D_2 receptors and 50% of D_3 receptors in rat striatum, and 5% of D_2 receptors and 78% of D_3 receptors in monkey striatum. These values can be derived from the saturation binding isotherm (i.e. Michaelis-Menten equation):

$$\frac{B}{B_{max}}=\frac{L}{L+K_d}, \quad (2)$$

where B is the specific receptor bound radioligand, B_{max} is the receptor density, L is the radioligand concentration, and K_d is the equilibrium dissociation constant. In this study, the L value was 4 nM and K_d values were 1.16 nM for D_3 and 76 nM for D_{2L} receptors in the monkey study, which were determined using binding data with cloned human receptors (Table I). In contrast, K_d values were 3.94 nM for D_3 and 158 nM for D_2 receptors in the rat brain study, which were determined from binding study with cloned rat receptors (Table I). With the same analysis and the binding data (Table I), 10 nM [^{3}H]raclopride will label a) 60% of D_2 receptors and 37% of D_3 receptors in rat striatum, and b) 86% of D_2 receptors and 36% of D_3 receptors in monkey striatum.

The total bound amount of receptors of 4.0 nM [^{3}H]**WC-10** or 10 nM [^{3}H]raclopride binding can be expressed by the formulas:

$$[^3\mathrm{H}]\mathbf{WC-10}: \quad a_1D_2+b_1D_3=B_1 \quad (3)$$

$$[^3\mathrm{H}]\text{raclopride}: a_2D_2+b_2D_3=B_2, \quad (4)$$

Where a_1 and b_1 are the fractional occupancies of 4nM of [^{3}H]**WC-10** to D_2 and D_3 receptors; B_1 is the apparent receptor binding density (D_2+D_3) directly measured from autoradiography studies of 4.0 nM of [^{3}H]**WC-10**; a_2, b_2, and B_2 are the same parameters for 10nM of [^{3}H]raclopride; D_2, D_3 are the absolute densities of D_2 and D_3 receptors. The absolute densities of D_2 and D_3 receptors were calculated by solving the simultaneous equations:

$$D_2=\frac{b_2B_1-b_1B_2}{a_1b_2-a_2b_1} \quad (5)$$

$$D_3=\frac{a_1B_2-a_2B_1}{a_1b_2-a_2b_1} \quad (6)$$

It's assumed that a) law of mass actions applies in this study; b) all receptors are equally accessible to both radioligands [^{3}H]**WC-10** and 10 nM [^{3}H]raclopride; c) both radioligands are antagonists and label high and low affinity sites of dopamine D_2 or D_3 receptors with equal affinity; d) neither receptor nor ligand are altered by binding; e) free radioligand concentration remains unchanged after binding.

RESULTS

Saturation experiments

Saturation experiments with genetically cloned receptors—Direct saturation binding studies were carried out using [^{3}H]**WC-10** and [^{3}H]raclopride with cloned human hD_3, hD_{2L} receptors on HEK cell membranes and rat rD_3, rD_{2L} receptors on Sf9 cell membranes. Detailed descriptions and data for [^{3}H]**WC-10** binding were reported

previously (Xu et al., 2009). The Scatchard plots and K_d values of [^{3}H]raclopride binding to human hD_3, hD_{2L} receptors expressed in HEK cells (Fig. 2A, B) and rat rD_3, rD_{2L} receptors expressed in Sf9 cell membranes (Fig. 2C, D) are shown in Figure 2. The K_d values of the receptor-radioligand binding of [^{3}H]**WC-10** and [^{3}H]raclopride to human and rat D_{2L}, D_3 receptors and their binding selectivity ratios are summarized (Table I). [^{3}H]**WC-10** binds with a 66-fold higher affinity to human HEK D_3 than to HEK D_{2L} receptors, with a dissociation constant (K_d) of 1.2 nM. [^{3}H]**WC-10** binds to rat Sf9 D_3 receptors with a K_d of 3.9 nM, demonstrating a 3-fold lower affinity for human HEK D_3 receptors and a 40-fold higher affinity for rat Sf9 D_{2L} receptors. [^{3}H]raclopride binds with a 11-fold higher affinity to human HEK D_{2L} (K_d = 1.6 nM) than to HEK D_3 (K_d = 18 nM) receptors; and [^{3}H]raclopride binds to rat Sf9 rD_{2L} receptors with a K_d of 6.79 nM, a value that is 4-fold lower than binding to human HEK D_{2L} receptors and 2.5-fold higher than binding to rat Sf9 rD_3 receptors. Because the average n_H values are close to unity, results indicate that receptor binding data fit well to one site model where the binding is non-cooperative.

Saturation experiments with rhesus monkey and rat brain sections—Direct saturation binding studies were conducted using [^{3}H]**WC-10** with rhesus monkey caudate (Fig. 3A), putamen (Fig. 3B) and rat caudate-putamen (Fig. 3C). The K_d and n_H values of the receptor-radioligand binding from Scatchard plots of [^{3}H]**WC-10** to rhesus monkey and rat caudate-putamen are shown in Figure 3. n_H values were close to equity, which suggest that the binding of [^{3}H]**WC-10** is to single binding site. [^{3}H]**WC-10** binds with dissociation constants (K_d s) of 1.3 and 1.1 nM to rhesus monkey caudate and putamen respectively. [^{3}H]**WC-10** binds to Sprague-Dawley rat striatum with dissociation constant (K_d) of 3.4 nM. Similar results of dissociation constants (K_d s) were also observed in Fisher 344 and Wistar rat brain (data not shown). These K_d values are in good accordance with the K_d values obtained from [^{3}H]**WC-10** binding to cloned human or rat receptors (Xu, et al., 2009). Therefore, the K_d values obtained from cloned receptors are suitable values for receptor occupancy estimates for the *in vitro* autoradiography of this study.

Quantitative autoradiography

Autoradiography showed that [^{3}H]**WC-10** and [^{3}H]raclopride labeled the D_2/D_3 sites in monkey striatal caudate and putamen, as well as the D_2/D_3 sites in rat striatum (Fig. 4 **A-D**). The sensitivity limit of Beta Imager 2000Z Digital Beta Imaging System was 0.07 dpm/mm^2. A tritium standard [^{3}H]Microscale (Figure 4E) with a series sections of known amount of radioactivity (ranging from 0.14 to 63.1 nCi/mg) was counted, and quantitative data analysis with Beta-Vision Plus yielded a ROI activity number ranging from 0.06 to 21.2 cpm/mm^2. These data were linearly fitted with a coefficient (R) greater than 0.99 (Fig. 5). This standard curve was used for calibration of tritium autoradiography of tissue sections, (i.e., converting cpm/mm into nCi/mg tissue) and the receptor bond radioligand densities were readily calculated utilizing the specific activities of radioligands.

Absolute dopamine D_2 and D_3 receptors densities from in vitro quantitative autoradiography

Based on the saturation binding analysis and the *in vitro* binding data of [^{3}H]**WC-10** and [^{3}H]raclopride to cloned human and rat D_2 and D_3 receptors, fractions of D_2 and D_3 receptor occupancies with 4 nM [^{3}H]**WC-10** and 10nM [^{3}H]raclopride binding in monkey and rat caudate-putamen are readily determined. The values of a_1, b_1, a_2, b_2, are summarized in Table II. With quantitative autoradiographic analysis, we measured the apparent receptor binding density (B_1s) of D_2 plus D_3 receptors using 4 nM [^{3}H]**WC-10** in monkey anterior caudate, putamen and rat striatum to be 125, 141 and 38 fmol/mg tissue respectively. The apparent receptor binding density (B_2s) of D_2 plus D_3 receptors in monkey caudate, putamen and rat striatum using 10 nM [^{3}H]raclopride are found to be 318, 345 and 145 fmol/mg

tissue respectively. With these receptor occupancy fraction numbers and the apparent receptor binding densities (B_1 and B_2 values), we obtained the absolute D_2 and D_3 receptors densities from equations (5) and (6). D_2 density were found to be about 310, 307 and 143 fmol/mg tissue for monkey caudate, putamen and rat striatum respectively, about 2.1~2.4 fold of D_3 densities. The apparent receptor binding densities of 4 nM [^{3}H]**WC-10** and 10 nM [^{3}H]raclopride, absolute D_2 and D_3 receptor densities (D_2 and D_3 values) and their density ratios (D_2/D_3) in rhesus monkey anterior caudate-putamen and rat striatum are summarized in Table III. With the same method, we calculated the absolute D_2 and D_3 receptor densities in monkey post anterior caudate-putamen where globus pallidus was present. We found that D_3 receptor density in post anterior striatum was lower than in anterior striatum and about one-fourth of D_2 receptor density (data not shown).

Comparison of digital Beta Imager autoradiography and film autoradiography

Autoradiograms of 4nM [^{3}H]**WC-10** incubated brain slides obtained with the traditional ^{3}H-Hyperfilm exposure techniques with different exposure period, 1 and 3 months, are shown in Figure 6. Although the image of 3-month exposure had a clear view of striatum and islands of Calleja, the image of 1-month exposure didn't show enough signal for visualization. While the digital Beta Imager can produce decent images for quantitative analysis after 24-hour acquisition (Figure 4), compared to traditional film autoradiography, the Biospace Beta Imager 2000Z Digital Beta Imaging System is a more sensitive, quantitative and higher-throughput tool for receptor autoradiography binding assays with tritium.

DISCUSSION

In a previous report (Xu et al., 2009), we have characterized D_3 receptor antagonist [^{3}H]**WC-10** and demonstrated it to be a high affinity and moderately selective radioligand for D_3 versus D_{2L} receptors using *in vitro* radioligand binding and autoradiography studies. **WC-10** was radiolabeled with tritium, and the *in vitro* binding of [^{3}H]**WC-10** to cloned dopamine D_{2L} and D_3 receptors was evaluated. [^{3}H]**WC-10** binds with a 66-fold higher affinity to human HEK D_3 than to HEK D_{2L} receptors, with a dissociation constant (K_d) of 1.2 nM. However, [^{3}H]**WC-10** binds to rat Sf9 rD_3 receptors with a K_d of 3.9 nM, a value that is 3-fold lower than binding to human HEK D_3 receptors and a 40-fold value higher than binding to rat Sf9 rD_{2L} receptors. *In vitro* autoradiography studies show that [^{3}H]**WC-10** labeled the majority of D_3 sites in the caudate and putamen for both adult rats and monkey brains.

In this comparative study, we characterized D_2 selective antagonist [^{3}H]raclopride binding properties to genetically cloned dopamine D_{2L} and D_3 receptors. [^{3}H]raclopride binds with a 11-fold higher affinity to human HEK D_{2L} (K_d = 1.6 nM) than to HEK D_3 (K_d = 18 nM) receptors, and [^{3}H]raclopride binds to rat Sf9 rD_{2L} receptors with a K_d of 6.79 nM, a value that is 4-fold lower than its binding to human HEK D_{2L} receptors and 2.5-fold higher than its binding to rat Sf9 rD_3 receptors. *In vitro* quantitative autoradiography studies with the combination of D_3/D_2 ligand, [^{3}H]**WC-10** and the D_2/D_3 ligand, [^{3}H]raclopride, were also conducted on adult rat and rhesus monkey brain sections. A mathematical model for calculating the absolute densities of dopamine D_2 and D_3 receptors based on the *in vitro* binding data obtained from [^{3}H]**WC-10** and [^{3}H]raclopride was also developed. Although it would be ideal to develop a more selective dopamine D_2 or D_3 receptor ligand for direct measurements of D_2 and D_3 receptors, the assay we presented in this paper permits an indirect evaluation of D_2 and D_3 receptor density ratios.

Although the D_3 receptor density was found to be lower (2.1–2.4-fold) than D_2 receptor density, and much lower (7–8-fold) than the dopamine D_1 receptor or vesicular monoamine transporter 2 (VMAT-2) density in the caudate putamen (unpublished data from our group),

the results presented here clearly show extensive binding of [^{3}H]**WC-10** in the caudate-putamen, which we believe represents binding to D_3 receptors. These results contradict the binding data obtained with the D_2/D_3 agonist, [^{3}H]7-OH-DPAT, but they are consistent with immunoprecipitation and immunofluoresence studies with antibodies demonstrating D_1 and D_3 heterodimerization, D_2 and D_3 receptors co-expression in the striatum (Ariano and Sibley, 1994; Boundy et al., 1993; Fauchey et al., 2000; Fiorentini et al., 2008; Marcellino et al., 2008; Schwartz et al., 1998). They are also in agreement with *in situ* hybridization studies showing extensive distribution of D_3 mRNA in the striatal tissue (Deransart et al., 2001; Joyce et al., 2004; Mihara et al., 2003; Quik et al., 2000). A D_3 knock-out mice binding study using the D_2/D_3 agonist [^{3}H]-(+)-PHNO (Rabiner et al., 2007) demonstrated a 50% reduction in ligand binding in the striatum of knock-out versus wild type mice, suggesting that D_2 and D_3 receptors are expressed with similar densities in the striatum (Yaroslavsky et al., 2006). Furthermore, *in vitro* autoradiography, radioligand binding and PET imaging studies also indicate that D_3 receptors are extensively expressed in the rat, cat, monkey and human striatums (Camacho-Ochoa et al., 1995; Joyce et al., 1998; Narendran et al., 2006; Neisewander et al., 2004; Rabiner et al., 2009; Silvers et al., 2006; Sweet et al., 2001; Wade et al., 2001; Wallace and Booze, 1995).

The D_2-like dopamine receptors (D_2, D_3, and D_4 receptors) are believed to be involved in the pathogenesis of several psychiatric and neurological disorders and they may play important roles in schizophrenia, Parkinson's disease and cocaine addiction. D_2 and D_3 receptors are regulated differently in these central nervous system (CNS) disorders (Abi-Dargham et al., 2000; Martinez et al., 2007; Ryoo et al., 1998; Staley and Mash, 1996). Due to the high amino acid homology and binding domain similarity of D_2 and D_3 receptors, development of highly selective ligands either to D_2 or D_3 receptors for direct evaluation of D_2 or D_3 receptors has been challenging. We have developed a unique procedure for determining absolute D_2 and D_3 receptor densities; this novel assay requires low radioactivity. Compared to traditional Scatchard saturation binding with multiple concentrations of single radioligand for measuring the receptor density, the method described in this paper took advantage of the less D_2 selective D_2/D_3 ligand [^{3}H]raclopride and novel moderately D_3 selective D_3/D_2 ligand [^{3}H]**WC-10.** This method represent a novel assay to indirectly evaluate D_2 and D_3 receptor densities with single concentrations of each radioligand. Our *in vitro* characterization and *in vivo* study showed that **WC-10** is a useful probe for investigating the role of dopamine D_3 receptors in behavioral pharmacology. The procedure generated here for measuring changes in absolute densities of dopamine D_3 and D_2 receptors can be utilized generally for the neuroscience community in investigating pathological and biological roles of D_3 and D_2 receptors in the variety of CNS disorders known to have an alteration in dopamine receptors.

With agonist binding studies, aging related or species related D_3 and D_2 receptor densities' dynamic changes were also reported (Flores et al., 1998; Levant, 1998). It's not well known if these alterations come from low and high affinity states exchanging or fresh receptor expressing. In the previous study (Xu et al., 2009), we demonstrated that **WC-10** can displace agonist [^{3}H]7-OH-DPAT binding in caudate and putamen. With the currently available agonist radiotracers and the novel antagonist binding assays we have described in this study, we would be able to quantitatively investigate the high and low affinity states of Dopamine D_2 and D_3 receptors for a better understanding of the alterations of these receptors and their significance in both health and disease. (Gonzalez and Sibley, 1995; Levant et al., 1993; Mukherjee et al., 2004; Sibley et al., 1982; Stanwood et al., 2000)

In summary, results from our studies indicate that [^{3}H]**WC-10** is an excellent radioligand for dopamine D_3 receptors *in vitro*. Its weak partial agonist properties make this a unique radiotracer for studying the anatomical distribution and the functional and biological roles of

dopamine D_3 receptors in neurological systems. Comparative studies with [^{3}H]**WC-10** and [^{3}H]raclopride using the mathematical model described here enable the indirect measurement of the absolute densities of D_2 and D_3 receptors. The mathematical model provided an excellent method for quantifying the D_2 and D_3 receptor density ratio, which would be valuable for general use for further investigating the pathological and pharmacological roles of dopamine receptors in neurological regulation.

Acknowledgments

We thank Terry Anderson and Deborah Carter for help with brain section preparation.

Contract grant sponsor: NIH; Contract grant numbers: DA12647, DA16181, NS048056 DA13584-03S1; Contract grant sponsor: NIH Shared Instrumentation Grant (The Beta Imager 2000Z Digital Beta Imaging System); Contract grant numbers: S10 RR021007).

References

Abi-Dargham A, Rodenhiser J, Printz D, Zea-Ponce Y, Gil R, Kegeles LS, Weiss R, Cooper TB, Mann JJ, Van Heertum RL, Gorman JM, Laruelle M. Increased baseline occupancy of D_2 receptors by dopamine in schizophrenia. Proc Natl Acad Sci USA. 2000; 97:8104–8109. [PubMed: 10884434]

Ariano MA, Sibley DR. Dopamine receptor distribution in the rat CNS: elucidation using anti-peptide antisera directed against D_{1A} and D_3 subtypes. Brain Research. 1994; 649:95–110. [PubMed: 7953659]

Boundy VA, Luedtke RR, Gallitano AL, Smith JE, Filtz TM, Kallen RG, Molinoff PB. Expression and characterization of the rat D_3 dopamine receptor: pharmacologic properties and development of antibodies. J Pharmacol Exp Ther. 1993; 264:1002–1011. [PubMed: 8437101]

Briand LA, Flagel SB, Seeman P, Robinson TE. Cocaine self-administration produces a persistent increase in dopamine D_2 High receptors. Eur Neuropsychopharmacol. 2008; 18:551–556. [PubMed: 18284941]

Camacho-Ochoa M, Walker EL, Evans DL, Piercey MF. Rat brain binding sites for pramipexole, a clinically useful D_3-preferring dopamine agonist. Neurosci Lett. 1995; 196:97–100. [PubMed: 7501268]

Chu W, Tu Z, McElveen E, Xu J, Taylor M, Luedtke RR, Mach RH. Synthesis and in vitro binding of N-phenyl piperazine analogs as potential dopamine D_3 receptor ligands. Bioorg Med Chem. 2005; 13:77–87. [PubMed: 15582454]

Deransart C, Landwehrmeyer GB, Feuerstein TJ, Lucking CH. Up-regulation of D_3 dopaminergic receptor mRNA in the core of the nucleus accumbens accompanies the development of seizures in a genetic model of absence-epilepsy in the rat. Brain Res Mol Brain Res. 2001; 94:166–177. [PubMed: 11597777]

Fauchey V, Jaber M, Caron MG, Bloch B, Le Moine C. Differential regulation of the dopamine D_1, D_2 and D_3 receptor gene expression and changes in the phenotype of the striatal neurons in mice lacking the dopamine transporter. Eur J Neurosci. 2000; 12:19–26. [PubMed: 10651856]

Fiorentini C, Busi C, Gorruso E, Gotti C, Spano P, Missale C. Reciprocal regulation of dopamine D_1 and D_3 receptor function and trafficking by heterodimerization. Mol Pharmacol. 2008; 74:59–69. [PubMed: 18424554]

Flores G, Wood GK, Barbeau D, Quirion R, Srivastava LK. Lewis and Fischer rats: a comparison of dopamine transporter and receptors levels. Brain Res. 1998; 814:34–40. [PubMed: 9838033]

Gehlert DR, Gackenheimer SL, Seeman P, Schaus J. Autoradiographic localization of [^{3}H]quinpirole binding to dopamine D_2 and D_3 receptors in rat brain. Eur J Pharmacol. 1992; 211:189–194. [PubMed: 1351846]

George SR, Watanabe M, Di Paolo T, Falardeau P, Labrie F, Seeman P. The functional state of the dopamine receptor in the anterior pituitary is in the high affinity form. Endocrinology. 1985; 117:690–697. [PubMed: 4017954]

Ginovart N, Galineau L, Willeit M, Mizrahi R, Bloomfield PM, Seeman P, Houle S, Kapur S, Wilson AA. Binding characteristics and sensitivity to endogenous dopamine of [^{11}C]-(+)-PHNO, a new

agonist radiotracer for imaging the high-affinity state of D_2 receptors in vivo using positron emission tomography. J Neurochem. 2006; 97:1089–1103. [PubMed: 16606355]

Gonzalez AM, Sibley DR. [^{3}H]7-OH-DPAT is capable of labeling dopamine D_2 as well as D_3 receptors. European Journal of Pharmacology. 1995; 272:R1–R3. [PubMed: 7713138]

Graff-Guerrero A, Mizrahi R, Agid O, Marcon H, Barsoum P, Rusjan P, Wilson AA, Zipursky R, Kapur S. The dopamine D_2 receptors in high-affinity state and D_3 receptors in schizophrenia: a clinical [^{11}C]-(+)-PHNO PET study. Neuropsychopharmacology. 2009; 34:1078–1086. [PubMed: 18987627]

Hillefors M, von Euler G. Pharmacology of [^{3}H]R(+)-7-OH-DPAT binding in the rat caudate-putamen. Neurochem Int. 2001; 38:31–42. [PubMed: 10913686]

Hillefors M, von Euler M, Hedlund PB, von Euler G. Prominent binding of the dopamine D_3 agonist [^{3}H]PD 128907 in the caudate-putamen of the adult rat. Brain Res. 1999; 822:126–131. [PubMed: 10082890]

Joyce JN, Myers AJ, Gurevich E. Dopamine D_2 receptor bands in normal human temporal cortex are absent in Alzheimer's disease. Brain Res. 1998; 784:7–17. [PubMed: 9518532]

Joyce JN, Woolsey C, Ryoo H, Borwege S, Hagner D. Low dose pramipexole is neuroprotective in the MPTP mouse model of Parkinson's disease, and downregulates the dopamine transporter via the D_3 receptor. BMC Biol. 2004; 2:22. [PubMed: 15473914]

Kaichi Y, Nonaka R, Hagino Y, Watanabe M. Dopamine D_3 receptor binding by D_3 agonist 7-OH-DPAT (7-hydroxy-dipropylaminotetralin) and antipsychotic drugs measured ex vivo by quantitative autoradiography. Can J Physiol Pharmacol. 2000; 78:7–11. [PubMed: 10741754]

King MV, Seeman P, Marsden CA, Fone KC. Increased dopamine D_{2High} receptors in rats reared in social isolation. Synapse. 2009; 63:476–483. [PubMed: 19217027]

Leff P. The two-state model of receptor activation. Trends Pharmacol Sci. 1995; 16:89–97. [PubMed: 7540781]

Levant B. Differential distribution of D_3 dopamine receptors in the brains of several mammalian species. Brain Res. 1998; 800:269–274. [PubMed: 9685676]

Levant B, Grigoriadis DE, DeSouza EB. [3H]quinpirole binding to putative D_2 and D_3 dopamine receptors in rat brain and pituitary gland: a quantitative autoradiographic study. J Pharmacol Exp Ther. 1993; 264:991–1001. [PubMed: 8437136]

Levesque D, Diaz J, Pilon C, Martres MP, Giros B, Souil E, Schott D, Morgat JL, Schwartz JC, Sokoloff P. Identification, characterization, and localization of the dopamine D_3 receptor in rat brain using 7-[3H]hydroxy-N,N-di-n-propyl-2-aminotetralin. Proc Natl Acad Sci U S A. 1992; 89:8155–8159. [PubMed: 1518841]

Luedtke RR, Freeman RA, Boundy VA, Martin MW, Huang Y, Mach RH. Characterization of ^{125}I-IABN, a novel azabicyclononane benzamide selective for D_2-like dopamine receptors. Synapse. 2000; 38:438–449. [PubMed: 11044891]

Luedtke RR, Mach RH. Progress in developing D_3 dopamine receptor ligands as potential therapeutic agents for neurological and neuropsychiatric disorders. Current Pharmaceutical Design. 2003; 9:643–671. [PubMed: 12570797]

Martinez D, Narendran R, Foltin RW, Slifstein M, Hwang DR, Broft A, Huang Y, Cooper TB, Fischman MW, Kleber HD, Laruelle M. Amphetamine-induced dopamine release: markedly blunted in cocaine dependence and predictive of the choice to self-administer cocaine. Am J Psychiatry. 2007; 164:622–629. [PubMed: 17403976]

Marcellino D, Ferre S, Casado V, Cortes A, Le Foll B, Mazzola C, Drago F, Saur O, Stark H, Soriano A, Barnes C, Goldberg SR, Lluis C, Fuxe K, Franco R. Identification of dopamine D_1-D_3 receptor heteromers. Indications for a role of synergistic D_1-D_3 receptor interactions in the striatum. J Biol Chem. 2008; 283:26016–26025. [PubMed: 18644790]

Mihara K, Kondo T, Suzuki A, Yasui-Furukori N, Ono S, Sano A, Koshiro K, Otani K, Kaneko S. Relationship between functional dopamine D_2 and D_3 receptors gene polymorphisms and neuroleptic malignant syndrome. Am J Med Genet B Neuropsychiatr Genet. 2003; 117B:57–60. [PubMed: 12555236]

Mukherjee J, Narayanan TK, Christian BT, Shi B, Yang ZY. Binding characteristics of high-affinity dopamine D_2/D_3 receptor agonists, 11C-PPHT and ^{11}C-ZYY-339 in rodents and imaging in non-human primates by PET. Synapse. 2004; 54:83–91. [PubMed: 15352133]

Narendran R, Frankle WG, Mason NS, Rabiner EA, Gunn RN, Searle GE, Vora S, Litschge M, Kendro S, Cooper TB, Mathis CA, Laruelle M. Positron emission tomography imaging of amphetamine-induced dopamine release in the human cortex: a comparative evaluation of the high affinity dopamine $D_2/_3$ radiotracers [^{11}C]FLB 457 and [^{11}C]fallypride. Synapse. 2009; 63:447–461. [PubMed: 19217025]

Narendran R, Slifstein M, Guillin O, Hwang Y, Hwang DR, Scher E, Reeder S, Rabiner E, Laruelle M. Dopamine ($D_2/_3$) receptor agonist positron emission tomography radiotracer [^{11}C]-(+)-PHNO is a D_3 receptor preferring agonist in vivo. Synapse. 2006; 60:485–495. [PubMed: 16952157]

Neisewander JL, Fuchs RA, Tran-Nguyen LT, Weber SM, Coffey GP, Joyce JN. Increases in dopamine D_3 receptor binding in rats receiving a cocaine challenge at various time points after cocaine self-administration: implications for cocaine-seeking behavior. Neuropsychopharmacology. 2004; 29:1479–1487. [PubMed: 15100700]

Neve KA, Seamans JK, Trantham-Davidson H. Dopamine receptor signaling. J Recept Signal Transduct Res. 2004; 24:165–205. [PubMed: 15521361]

Quik M, Police S, He L, Di Monte DA, Langston JW. Expression of D_3 receptor messenger RNA and binding sites in monkey striatum and substantia nigra after nigrostriatal degeneration: effect of levodopa treatment. Neuroscience. 2000; 98:263–273. [PubMed: 10854757]

Rabiner E, Raymond R, Diwan M, McCormick P, Wilson A, Nobrega J. D_3 and D_2 components of ex vivo regional (+)-PHNO brain binding in wild-type and knock-out mice. J nucl med meeting abstracts. 2007; 48:113P-b.

Rabiner EA, Slifstein M, Nobrega J, Plisson C, Huiban M, Raymond R, Diwan M, Wilson AA, McCormick P, Gentile G, Gunn RN, Laruelle MA. In vivo quantification of regional dopamine-D_3 receptor binding potential of (+)-PHNO: Studies in non-human primates and transgenic mice. Synapse. 2009; 63:782–793. [PubMed: 19489048]

Ryoo HL, Pierrotti D, Joyce JN. Dopamine D_3 receptor is decreased and D_2 receptor is elevated in the striatum of Parkinson's disease. Mov Disord. 1998; 13:788–797. [PubMed: 9756147]

Schwartz JC, Diaz J, Bordet R, Griffon N, Perachon S, Pilon C, Ridray S, Sokoloff P. Functional implications of multiple dopamine receptor subtypes: the D_1/D_3 receptor coexistence. Brain Res Brain Res Rev. 1998; 26:236–242. [PubMed: 9651537]

Sibley DR, De Lean A, Creese I. Anterior pituitary dopamine receptors. Demonstration of interconvertible high and low affinity states of the D_2 dopamine receptor. J Biol Chem. 1982; 257:6351–6361. [PubMed: 6176582]

Silvers JM, Wallace DR, Harrod SB, Mactutus CF, Booze RM. Prenatal cocaine alters dopamine and sigma receptor binding in nucleus accumbens and striatum in dams and adolescent offspring. Neurotoxicol Teratol. 2006; 28:173–180. [PubMed: 16529908]

Skinbjerg M, Namkung Y, Halldin C, Innis RB, Sibley DR. Pharmacological characterization of 2-methoxy-N-propylnorapomorphine's interactions with D_2 and D_3 dopamine receptors. Synapse. 2009; 63:462–475. [PubMed: 19217026]

Staley JK, Mash DC. Adaptive increase in D_3 dopamine receptors in the brain reward circuits of human cocaine fatalities. J Neurosci. 1996; 16:6100–6106. [PubMed: 8815892]

Stanwood GD, Artymyshyn RP, Kung MP, Kung HF, Lucki I, McGonigle P. Quantitative autoradiographic mapping of rat brain dopamine D_3 binding with [^{125}I]7-OH-PIPAT: evidence for the presence of D_3 receptors on dopaminergic and nondopaminergic cell bodies and terminals. J Pharmacol Exp Ther. 2000; 295:1223–1231. [PubMed: 11082459]

Sweet RA, Hamilton RL, Healy MT, Wisniewski SR, Henteleff R, Pollock BG, Lewis DA, DeKosky ST. Alterations of striatal dopamine receptor binding in Alzheimer disease are associated with Lewy body pathology and antemortem psychosis. Arch Neurol. 2001; 58:466–472. [PubMed: 11255451]

Vasdev N, Seeman P, Garcia A, Stableford WT, Nobrega JN, Houle S, Wilson AA. Syntheses and in vitro evaluation of fluorinated naphthoxazines as dopamine D_2/D_3 receptor agonists:

radiosynthesis, ex vivo biodistribution and autoradiography of [^{18}F]F-PHNO. Nucl Med Biol. 2007; 34:195–203. [PubMed: 17307127]

Wade TV, Rothblat DS, Schneider JS. Changes in striatal dopamine D_3 receptor regulation during expression of and recovery from MPTP-induced parkinsonism. Brain Research. 2001; 905:111–119. [PubMed: 11423085]

Wallace DR, Booze RM. Identification of D_3 and sigma receptors in the rat striatum and nucleus accumbens using (+/−)-7-hydroxy-N,N-di-n-[3H]propyl-2-aminotetralin and carbetapentane. J Neurochem. 1995; 64:700–710. [PubMed: 7830063]

Xu J, Chu W, Tu Z, Jones LA, Luedtke RR, Perlmutter JS, Mintun MA, Mach RH. [(3)H]4-(Dimethylamino)-N-[4-(4-(2-methoxyphenyl)piperazin-1-yl)butyl]benzamide, a selective radioligand for dopamine D_3 receptors. I. In vitro characterization. Synapse. 2009; 63:717–728. [PubMed: 19425052]

Yaroslavsky I, Colletti M, Jiao X, Tejani-Butt S. Strain differences in the distribution of dopamine (DA_2 and DA_3) receptor sites in rat brain. Life Sci. 2006; 79:772–776. [PubMed: 16574158]

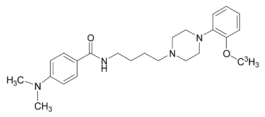

Fig. 1. Chemical structure of [^{3}H]WC-10

The structure of [^{3}H]**WC-10** are shown, detailed synthesis scheme was reported previously (Xu et al., 2009).

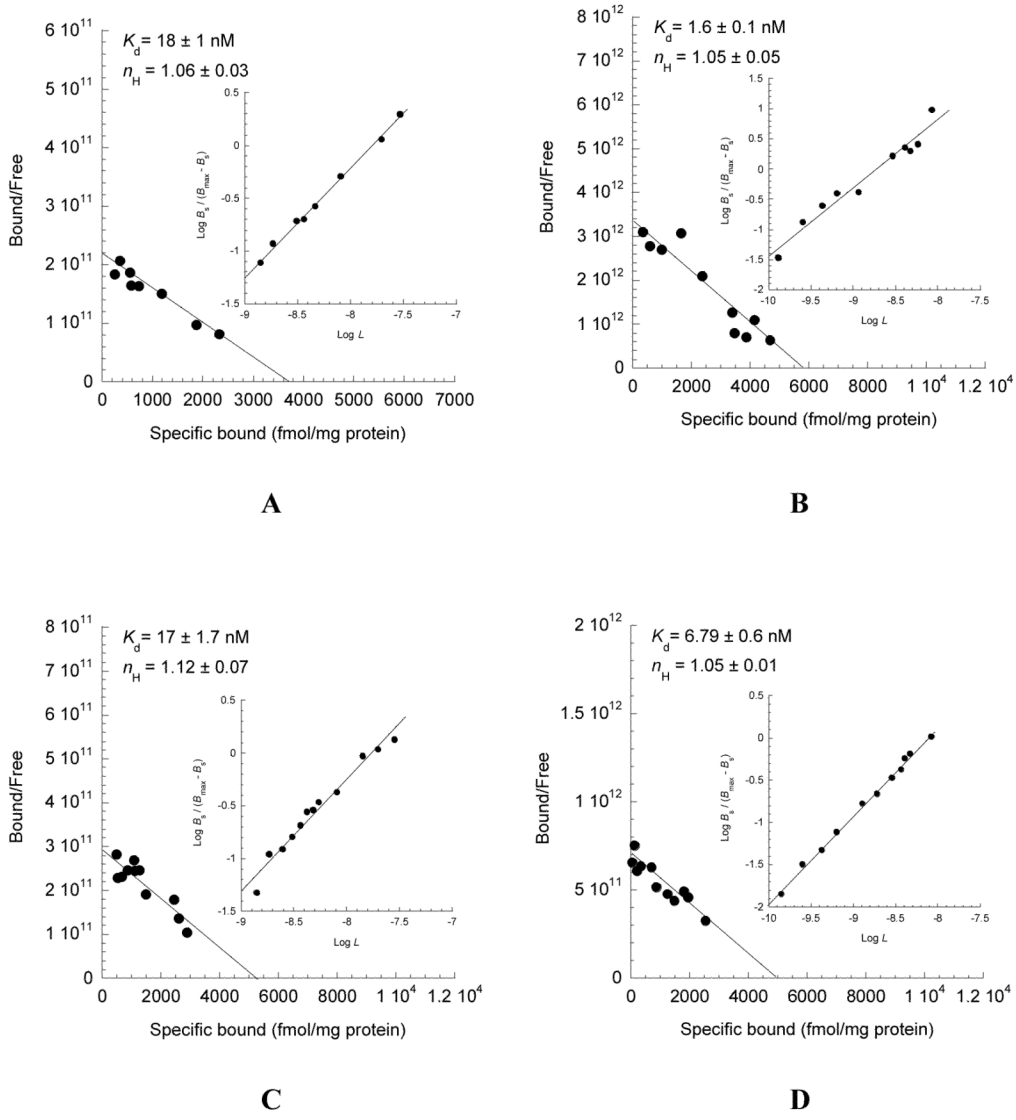

Fig. 2. Saturation analysis of the binding of [^{3}H]raclopride to cloned D_2-like dopamine receptors

Direct binding analysis was performed to determine the equilibrium binding affinity of [^{3}H]raclopride for human hD_3 and hD_2 (**A, B**) or rat rD_3 and rD_2 (**C, D**) receptors. Human receptors were expressed in HEK 293 cells and the rat receptors were expressed in Sf9 cells. Scatchard plots were used to determine the dissociation constants (K_d values). The inset graphs are the Hill plots for determining the Hill coefficient (n_H values). K_d and n_H are presented as mean values ± S.E.M for n = 3.

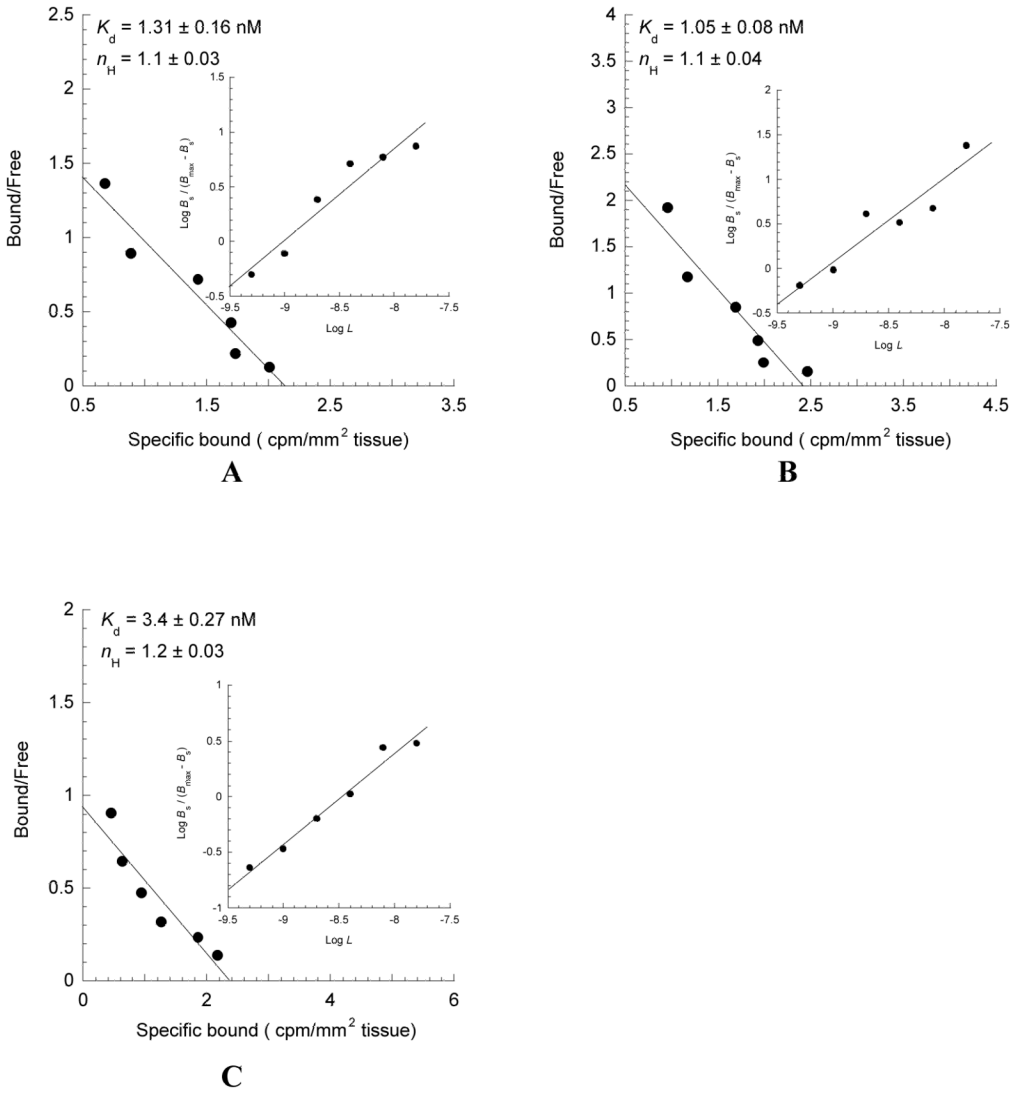

Fig. 3. Saturation analysis of the binding of [^{3}H]WC-10 to rhesus monkey and rat brain

Direct binding analysis was performed to determine the equilibrium binding affinity of [^{3}H]**WC-10** binding sites in the rhesus monkey caudate (graph **A**), putamen (graph **B**) and rat striatum (graph **C**). Nonspecific binding was determined from samples which contained 1 uM S(−)-Eticlopride. Scatchard plots were used to determine the dissociation constants (K_d values). The inset graphs are the Hill plots for determining the Hill coefficient (n_H values). K_d and n_H are presented as mean values ± S.E.M for n = 3.

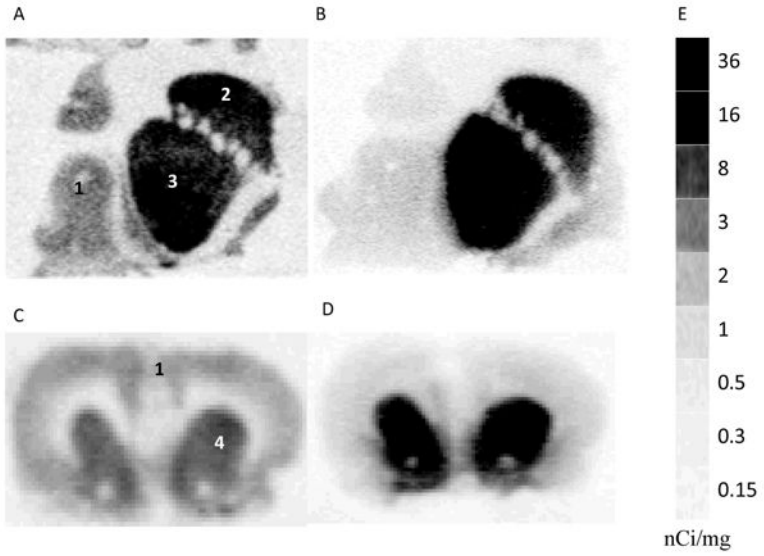

Fig. 4. Quantitative autoradiographic analysis of the binding of [^{3}H]WC-10 and [^{3}H]raclopride to rat and rhesus monkey brain

Autoradiograms show neuroanatomical localization of [^{3}H]**WC-10** and [^{3}H]raclopride binding sites in rhesus monkey (**A, B**) and Sprague-Dawley rat (**C, D**) brain sections. For this study [^{3}H]**WC-10** was used at a concentration of 4 nM (**A, C**) and [^{3}H]raclopride was used at a concentration of 10 nM (**B, D**). The numbers 1 through 4 in panels **A** and **C** designate the following CNS anatomical regions: 1) cortex, 2) primate caudate, 3) primate putamen and 4) rat striatum. Panel **E** shows autoradiographic image of a [^{3}H]Microscale, which was counted for 24 hours along with the brain sections for the purpose of quantitative analysis.

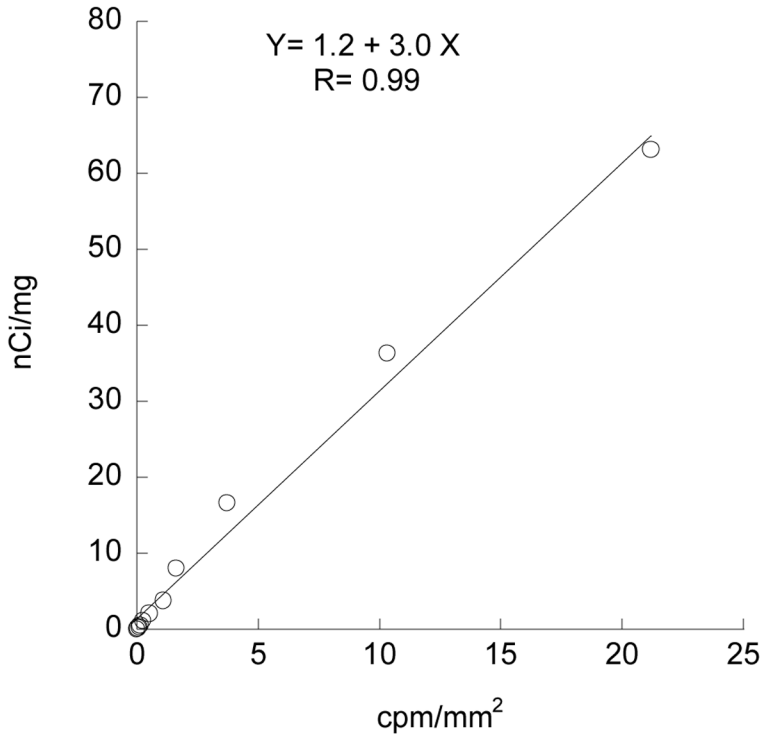

Fig. 5. Quantitative calibration of *in vitro* autoradiography

Calibrated autoradiography standard typical curve obtained by counting a series of tritium standards of a [^{3}H]Microscale, digitalized image was used to analyze the region of interest. This curve was used to convert cpm/mm^2 to nCi/mg to quantify autoradiography.

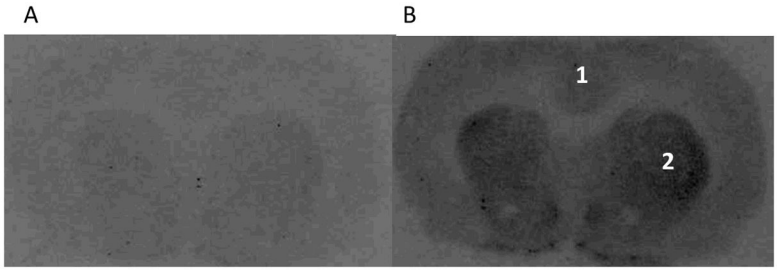

Fig. 6. Film autoradiography of the binding of [^{3}H]WC-10 to rat brain

Autoradiograms obtained with the traditional film exposure techniques with different exposure time, **A**. 1 month; **B**, 3 months. The numbers 1 and 2 designate the following CNS anatomical regions: 1) cortex, 2) rat striatum. For this study [^{3}H]**WC-10** was used at a concentration of 4 nM.

TABLE I

Dissociation constants (K_d values) of [^{3}H]WC-10 and [^{3}H]raclopride binding to dopamine D_2 and D_3 receptors

Receptors	Radioligand	
	[^{3}H]WC-10*	**[^{3}H]raclopride**
hD_{2L}	76 ± 4	1.6 ± 0.1
hD_3	1.16 ± 0.1	18 ± 1
D_{2L}/D_3	65.5	0.09
rD_{2L}	158 ± 8.3	6.79 ± 0.6
rD_3	3.94 ± 0.19	17.1 ± 1.7
D_{2L}/D_3	40.1	0.4

K_d values (nM), presented as mean value ± S.E.M for n=3, were obtained through saturation binding of [^{3}H]**WC-10** and [^{3}H]raclopride to a: cloned human D_3 and D_{2L} receptors expressed in HEK cells and b: rat D_3, D_{2L} receptors expressed in Sf9 cells.

*Data were taken from Xu et. al., 2009

TABLE II

Fractions of D_2 and D_3 receptors occupancy

	a_1	b_1	a_2	b_2
Monkey	0.05	0.78	0.86	0.36
Rat	0.02	0.5	0.6	0.37

a_1, b_1, a_2, and b_2 represents the receptors occupancy fractions of 4 nM [^{3}H]**WC-10** and 10 nM [^{3}H]raclopride binding to dopamine D_2 and D_3 receptors in the monkey and rat striatum. These values were derived from the saturation binding isotherm, equation (2), using the K_d values in Table I.

TABLE III

Absolute D_2 and D_3 receptor densities density ratios in rhesus monkey caudate, putamen and rat striatum

	B_1 fmol/mg Tissue	**B_2 fmol/mg Tissue**	**D_2 fmol/mg Tissue**	**D_3 fmol/mg Tissue**	**D_2:D_3**
Rhesus caudate	125 ± 3	318 ± 17	310 ± 21	141 ± 2	2.20 ± 0.16
Rhesus putamen	141 ± 4	345 ± 23	307 ± 30	130 ± 5	2.36 ± 0.2
Rat striatum	38 ± 2	145 ± 4	143 ± 7	68 ± 3	2.11 ± 0.23

Apparent binding densities (B_1 and B_2) of 4 nM [^{3}H]**WC-10** and 10 nM [^{3}H]raclopride were directly measured with quantitative autoradiography; absolute D_2 and D_3 receptor densities and the receptor density ratios D_2:D_3 were calculated from the equations (5) and (6) using the a_1, b_1, a_2, and b_2 values in the Table II and the B_1, B_2 values in this Table. Data were presented as mean value ± S.E.M, n=8 for rhesus monkey caudate-putamen and n=30 for rat striatum.